Biochemical and Biophysical Research Communications 430 (2013) 301–306

Contents lists available at SciVerse ScienceDirect

Biochemical and Biophysical Research Communications

journal homepage: www.elsevier.com/locate/ybbrc

Visualization of cyclooxygenase-2 using a 2,3-diarylsubstituted indole-based inhibitor and confocal laser induced cryofluorescence microscopy at 20 K in melanoma cells *in vitro*

Christoph Tondera [a,c], Markus Laube [a,c], Christin Wimmer [a,c], Torsten Kniess [a], Birgit Mosch [a], Kay Großmann [b], Jens Pietzsch [a,c,*]

[a] Institute of Radiopharmacy (From January 2013 Institute of Radiopharmaceutical Cancer Research), Helmholtz-Zentrum Dresden-Rossendorf, Germany
[b] Institute of Resource Ecology, Helmholtz-Zentrum Dresden-Rossendorf, Germany
[c] Technische Universität Dresden, Dresden, Germany

ARTICLE INFO

Article history:
Received 29 October 2012
Available online 9 November 2012

Keywords:
Coxibs
Tumor inflammogenesis
Pigment cells
Fluorescence imaging

ABSTRACT

This study aimed at visualization of cyclooxygenase-2 (COX-2) protein expression in melanoma cells by confocal laser induced cryofluorescence microscopy using 4-(3-(4-methoxyphenyl)-*1H*-indol-2-yl)benzene-sulfonamide (C1) representative for a novel class of autofluorescent 2,3-diarylsubstituted indole-based selective COX-2 inhibitors.

COX-2 expression was measured in human melanoma cell lines A2058 and MelJuso by immunocytochemistry and immunoblotting. Cellular uptake experiments using varying C1 concentrations down to 0.1 nM (with/without molar excess of celecoxib as control) were performed at 37 °C. Cryofluorescence microscopy was conducted at 20 K.

COX-2 protein expression was successfully visualized by C1 in A2058 cells. COX-2-negative MelJuso cells showed no specific accumulation of C1. Control experiments using celecoxib and, additionally, implemented fluorescence spectroscopy confirmed specificity of both cellular uptake and intracellular association of C1.

Cryofluorescence microscopy in combination with spectroscopy allowed for visualization of COX-2 protein expression in melanoma cells *in vitro* using a selective COX-2 inhibitor at very low concentrations.

1. Introduction

Cyclooxygenase-2 (COX-2) is an inducible enzyme, whose overexpression is implicated in a number of inflammatory disease processes. Furthermore, an elevated COX-2 level is a prominent finding in most of human epithelium-derived malignant tumors and is correlated with tumor inflammogenesis, progression, metastasis, and radiosensitivity [1]. Human melanoma, a non-epithelial tumor characterized by a marked inflammatory response and widespread metastasis, also overexpresses COX-2 [2]. As shown by immunohistochemistry, COX-2 expression in primary melanomata is restricted to melanoma cells and significant correlation between immunohistochemical staining, tumor thickness, and disease-specific survival has been reported. In this regard, COX-2 has been suggested a prognostic marker and a potential therapeutic target in melanoma [3]. Consequently, blocking the COX-2 isoenzyme selectively may provide an effective chemopreventive or adjuvant radiosensitizing therapy. In this regard, novel selective COX-2 inhibitors (coxibs) based on a 2,3-diarylsubstituted indole chemical lead with high affinity and selectivity recently have been developed as both promising therapeutic compounds and important templates for radiotracer design by others [4] and us [1]. Visualizing COX-2 protein expression *in vitro* and *in vivo*/*ex vivo* is suggested an important approach to follow tumor progression and monitor the effects of therapeutic interventions. In this regard, the 2,3-diarylsubstituted indoles exhibit physicochemical properties suggesting them to be promising fluorescent tracers *in vitro* and *in vivo*. In this paper we report the use of 4-(3-(4-methoxyphenyl)-*1H*-indol-2-yl)benzene-sulfonamide at very low concentrations for visualization of COX-2 protein expression *in vitro* by confocal laser induced cryofluorescence microscopy in melanoma cells.

Abbreviations: BSA, bovine serum albumin; COX-2, cyclooxygenase-2; FCS, fetal calf serum; PBS, phosphate buffered saline; TPA, tetradecanoyl phorbol acetate.

* Corresponding author at: Institute of Radiopharmacy, Helmholtz-Zentrum Dresden-Rossendorf, Dresden, Germany.
E-mail address: j.pietzsch@hzdr.de (J. Pietzsch).

0006-291X/$ - see front matter © 2012 Elsevier Inc. All rights reserved.
http://dx.doi.org/10.1016/j.bbrc.2012.10.133

2. Materials and methods

2.1. Chemical synthesis

Selective COX-2 inhibitors 4-(3-(4-methoxyphenyl)-*1H*-indol-2-yl)benzene-sulfonamide (C1) and 4-[5-(4-methylphenyl)-3-(trifluoromethyl)pyrazol-1-yl]benzenesulfonamide (celecoxib) were synthesized according to the methods published by Hu et al. [4] and Penning et al. [5]. Analysis of fluorescence properties was conducted using the Synergy™ 4 multi-mode microplate reader (Bio-Tek Instruments, Bad Friedrichshall, Germany). At first a 10 mM stock solution of C1 in DMSO was prepared. The measurements were done in 96 well plates in an aqueous environment. Therefore the stock solution was diluted (1:100) in phosphate buffered saline (PBS) with additional 1% Tween 20. The final concentration of C1 was 100 μM. Furthermore the quantum yield of C1 was analyzed. Therefore the fluorescence intensity and the absorption of C1 were associated to the same properties of a fluorescence dye (Hoechst 33258) with known quantum yield and similar excitation and emission maxima in the same solvent as described above. The quantum yield was calculated according to formula 1 with $\varphi_{A/B}$, quantum yield of substance *A*/*B*; $I_{A/B}$, integrated fluorescence emission intensity area from excitation wavelength +30 nm to 800 nm of substance *A*/*B*; $A_{A/B}$, optical density of substance *A*/*B* at excitation wavelength and $\eta_{A/B}$, the reflective index of substance *A*/*B*. For simplification and because both substances were measured in the same solvent, the term regarding the reflective index η was defined to be 1 [6].

$$\frac{\Phi_A}{\Phi_B} = \frac{I_A * A_B * n_A^2}{I_B * A_A * n_B^2} \quad (1)$$

The quantum yield of Hoechst 33258 in an aqueous solvent is 3.4% [7].

2.2. Cryofluorescence spectroscopy

To analyze the fluorescence intensity of C1 at different temperatures a 1 nM solution of C1 was prepared and spectroscopically measured both at room temperature and at 20 K. Because of the low concentration the substance could be completely dissolved in MilliQ water (MilliQ PF Plus System, Millipore, Eschborn, Germany) without any supplements. The sample was excited using an Inlite II Laser (Continuum, Santa Clara, USA) with a wavelength of 266 nm. For detection a SpectraPro 300i spectrograph (Princeton Instruments, Acton, USA) and an ICCD-Camera (Princeton Instruments, Stuttgart, Germany) were used. Cryogenic temperatures were achieved using an adiabatic helium cooling system (Refrigerator gekühltes Kryostat RDK 10-320; Ultrapumpstand PT50 KIT/DN 40KF and Kompressionseinheit RW2, Oerlicon Leybold, Dresden, Germany).

2.3. Cell culture

The amelanotic human malignant melanoma cell lines A2058 and MelJuso were cultivated as described elsewhere [8]. For experiments 5×10^4 cells (passages 5–15) were seeded in chamber slides and grown overnight to confluence of 50%.

2.4. Analysis of COX-2 protein expression

The seeded cells were fixed for 30 min at 4 °C with 4% paraformaldehyde and for 10 min at −20 °C with methanol. Then cells were treated with 0.3% Triton X-100 in PBS to make them permeable and with 5% bovine serum albumin (BSA) in PBS to block unspecific binding sites. The cells were incubated overnight with the primary anti-COX-2 antibody (M-19, sc-1747, 1:50, SantaCruz Biotechnology, Heidelberg, Germany) in 0.1% Tween 20 in PBS and without the primary antibody as negative control. Afterwards all cells were incubated with the secondary antibody conjugate Alexa Fluor 594® (Molecular Probes®, Darmstadt, Germany) for 60 min. Counterstaining was done with the DNA dye Hoechst 33258 (Molecular Probes®) for 5 min at a concentration of 2 μg/ml. The cells were dehydrated and conserved using an ethanol gradient. The slides were measured at the Axio Imager A1 (Carl Zeiss MicroImaging, Jena, Germany, setup for Hoechst 33258: λ_{Ex} = 365 nm, λ_{Em} = BP 445/50 nm; setup for Alexa Fluor 594®: λ_{Ex} = 575–640 nm; λ_{Em} = BP 549/12 nm). The bright field and the fluorescence images were merged using the program Axio Vision (Carl Zeiss MicroImaging). Moreover, COX-2 protein expression was characterized by Western blot analysis with the same primary anti-COX-2 antibody as published elsewhere [1].

2.5. Confocal laser induced cryofluorescence microscopy

The seeded cells were incubated for 2 h with different concentrations of C1 dissolved in medium with and without a pre-incubation for 1 h of 10 μM celecoxib. After incubation the cells were fixed for 30 min at 4 °C with 4% paraformaldehyde and for 10 min at −20 °C with methanol. The counterstaining was performed with the membrane dye 5-N-hexadecanoylaminofluorescein (5-hex, Molecular Probes®) for 15 min at a concentration of 5 μM and the DNA dye SYTO 59 (Molecular Probes®) for 30 min at a concentration of 10 μM. After staining the cells were rinsed with PBS and hermetically embedded. The prepared slides (original and counterstained) were measured with the confocal laser scanning microscope Leica TCS SP2 (Leica Microsystems, Wetzlar, Germany) using an argon UV laser (351 nm, 364 nm; Coherent, Santa Clara, USA) to excite the 2,3-diarylsubstituted indole-based COX-2 inhibitor (C1), an argon laser (496 nm; Leica) to excite the membrane stain, and an helium neon laser (633 nm; Leica Microsystems) to excite the DNA stain. Analysis was performed both at room temperature and at 20 K. Cryogenic temperatures were achieved by using a special Gifford–McMahon-type based closed cycle helium cooling system for light microscopic applications (NanoscopiX, Dresden, Germany). The sample chamber is characterized by special geometry for a simple adaption on commercial fluorescence microscopes. A silica glass window was used to lead the beam path onto the slide into the vacuum sample chamber [9]. The fluorescence images were merged using the Leica Confocal Software.

3. Results and discussion

In this pilot study the selected compound C1 was investigated as a representative for a novel class of fluorescent 2,3-diarylsubstituted indole-based selective coxibs. Former radiotracer experiments using a fluorine-18-radiolabeled analog of C1 demonstrated its *in vitro* cellular uptake and intracellular association in various tumor and inflammatory cells consistent to the published COX-1/COX-2 selectivity and well correlated to the observed protein expression of cyclooxygenase isoforms in these cells [1]. Fig. 1A shows the structure of C1 and the corresponding fluorescence spectrum. Besides its spectral properties C1 also exhibits a relatively high quantum yield (5.2%) compared to other members of this class of compounds (data not shown in detail). Fig. 2 shows the different extent of COX-2 protein expression in human malignant melanoma cell lines A2058 and MelJuso, respectively, as determined by both Western blot analysis and immunocytochemical staining. A2058 cells show a high COX-2 protein level with the enzyme chiefly located around the nucleus. This finding

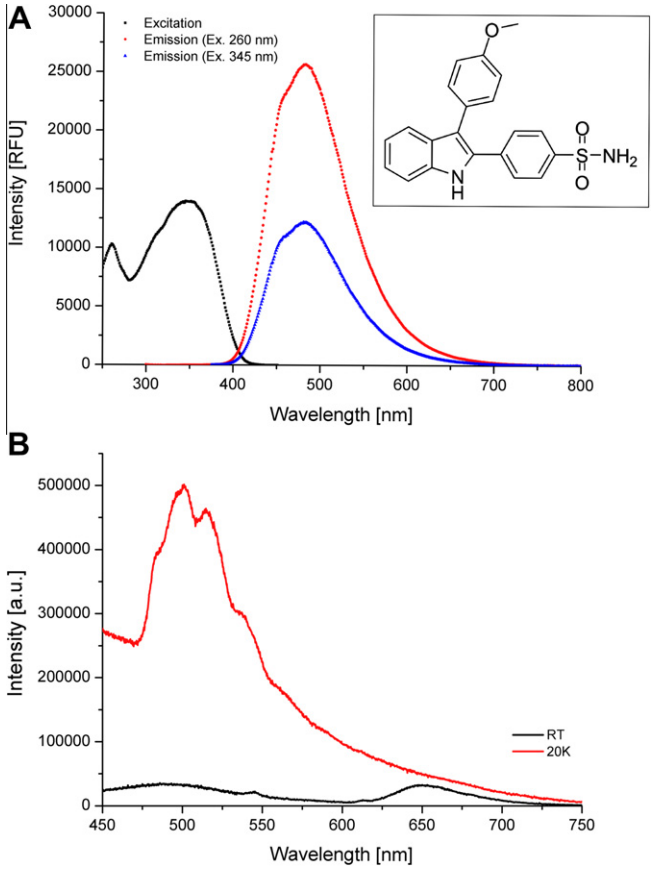

Fig. 1. Structure, excitation and emission spectra of C1. (A) Excitation spectrum and emission spectra at both excitation maxima wavelengths of 100 μM C1 measured at room temperature using the Synergy™ 4 multi-mode microplate reader. (B) Emission spectrum of 1 nM C1 in H_2O measured at both room temperature and 20 K using a SpectraPro 300i spectrograph and an ICCD-Camera. For excitation an Inlite II Laser with a wavelength of 266 nm was used.

is consistent with the literature reporting localization of COX-2 in the nuclear envelope and in the lumen of the endoplasmic reticulum [10,11]. In contrast, MelJuso cells showed no detectable COX-2 and, therefore, were used as negative control. After cellular uptake of C1, studied at very low concentrations (0.1–1.0 nM), confocal scanning laser microscopy was performed at room temperature and at 20 K. At room temperature no or only weak fluorescence emission signal of C1 was detectable by the microscope used. Therefore, cryofluorescence microscopy at 20 K was applied. In contrast to measurements at room temperature, at 20 K C1 showed suitable signal intensity for COX-2 visualization in melanoma cells (Fig. 3). This observation is consistent with the observed substantial increment in signal intensity of 1 nM C1 at cryogenic temperature compared to room temperature as measured by cryofluorescence spectroscopy (Fig. 1B).

The cellular uptake of C1 in melanoma cells well correlates with the COX-2 expression pattern (Fig. 3). For better mapping of COX-2 the nuclei and membranes were counterstained with specific dyes (Fig. 3). In A2058 cells an enrichment of C1 around the nucleus can be observed (Fig. 3A). If the study is repeated with the same cell line but after a pre-incubation with molar excess (10 μM) celecoxib for 1 h this local accumulation of C1 cannot be observed (Fig. 3B). Moreover, fluorescence intensity is substantially lower in cells pre-incubated with celecoxib compared to cells incubated without celecoxib as demonstrated in spectral analysis (Fig. 4). The spectrum shows two emission peaks at an excitation wavelength of 351 nm. The first peak with

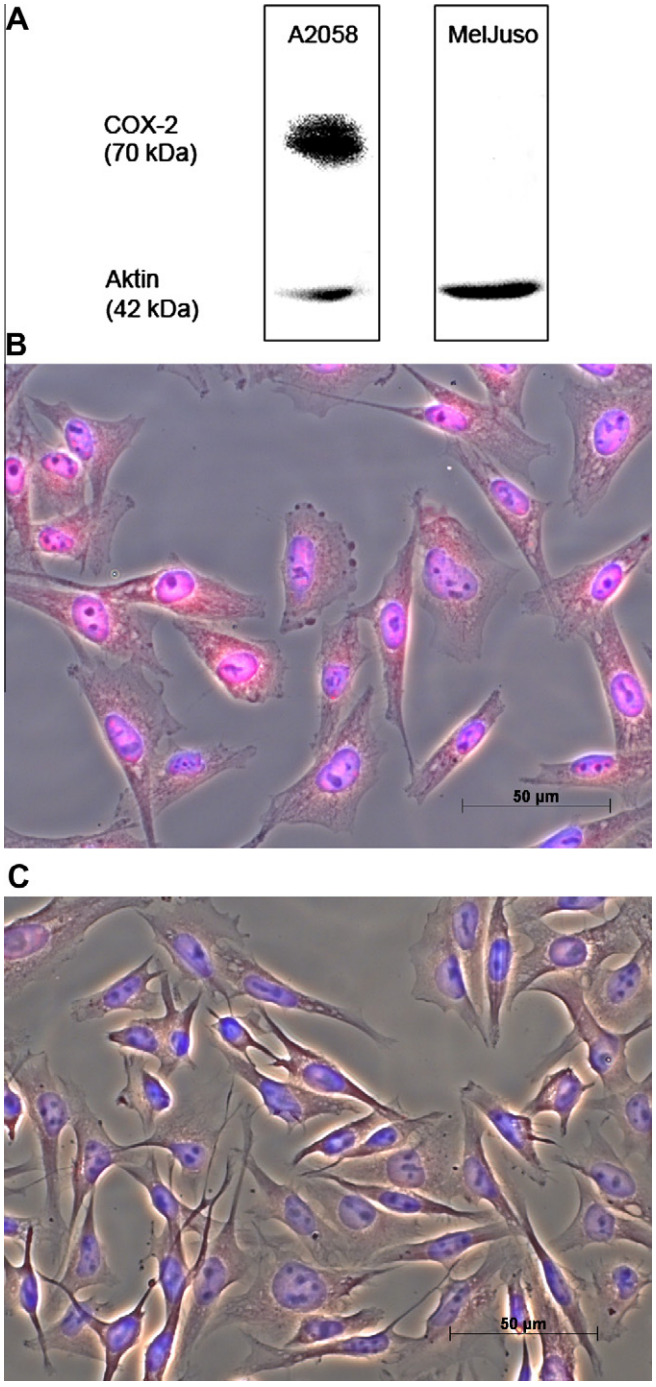

Fig. 2. COX-2 protein expression in human melanoma cell lines A2058 and MelJuso. Western blot analysis in (A) both cell lines, and immunocytochemical analysis in (B) A2058 cells and (C) MelJuso cells, respectively. The bright field image showing COX-2 staining using primary anti COX-2 antibody/secondary Alexa Fluor 594® antibody conjugate (red) was merged with the Hoechst 33258 DNA staining (blue).

a maximum at about 480 nm well correlates with the emission maximum of the C1. The second peak at about 510 nm correlates with the emission maximum of the membrane stain 5-hex (Fig. 4). In comparison to these results the cellular uptake of C1 in MelJuso cells showed another characteristic. No specific enrichment of C1 around the nucleus could be observed (Fig. 3C). However, there is a fluorescence signal of C1 detectable in MelJuso cells. But in comparison to measurement of the

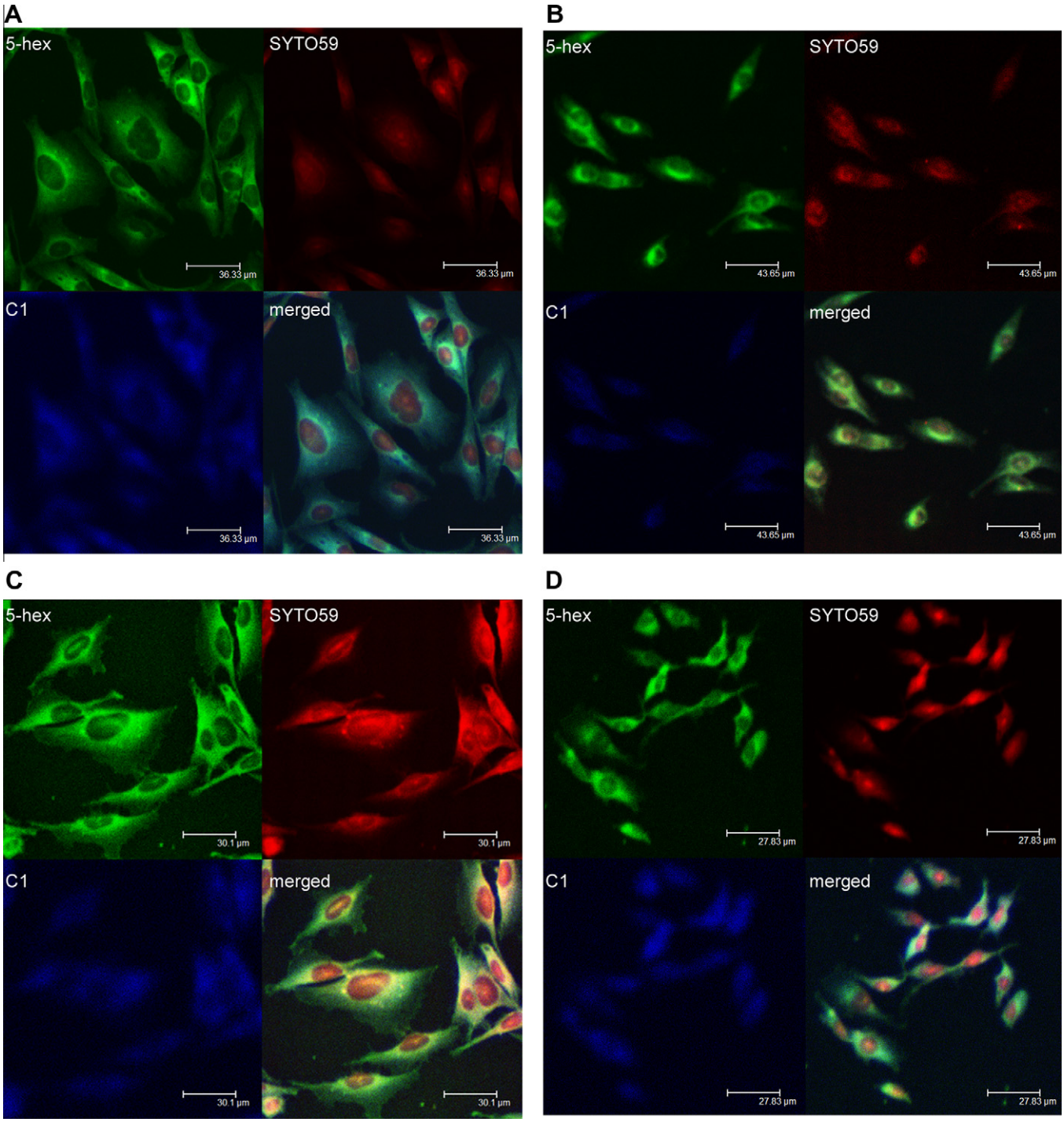

Fig. 3. Visualization of COX-2 protein expression by cryofluorescence microscopy at 20 K after cellular uptake of C1 in A2058 and MelJuso cells. A2058 (A and B) and MelJuso (C and D) cells were incubated for 2 h at 37 °C with 1 nM C1 without celecoxib (A and C) and with 10 µM celecoxib (B and D), respectively. Additionally, after cellular uptake of different concentrations of C1 (0.5 nM (E); 0.1 nM (F), and 0.1 nM with open pinhole (G)) in A2058 cells incubated for 2 h at 37 °C without celecoxib cryofluorescence microscopy at 20 K was performed.

cellular uptake of C1 in A2058 cells a signal gain had to be applied even to detect fluorescence with good intensity. In MelJuso cells C1 is unspecifically distributed over the whole cell. The distribution of the signal is comparable with that observed in A2058 cells pre-incubated with celecoxib (Fig. 3D). Since the method showed reliable data in visualizing COX-2 using 1 nM of C1, different lower concentrations were tested. Of importance, at a concentration of 0.5 nM of C1 there was still a fluorescence signal detectable around the nucleus. Using a concentration of 0.1 nM C1 there was no signal detectable in a confocal volume (1 Airy). However, after the pinhole was opened the enrichment of the inhibitor could be detected again by cryofluorescence microscopy, by accepting diminishment of resolution in *z*-direction (Fig. 3E–G).

In summary, this study demonstrates first visualization of COX-2 protein expression in melanoma cells with a fluorescent selective COX-2 inhibitor using cryofluorescence microscopy at 20 K. Compared with the work of other groups [12,13], who used

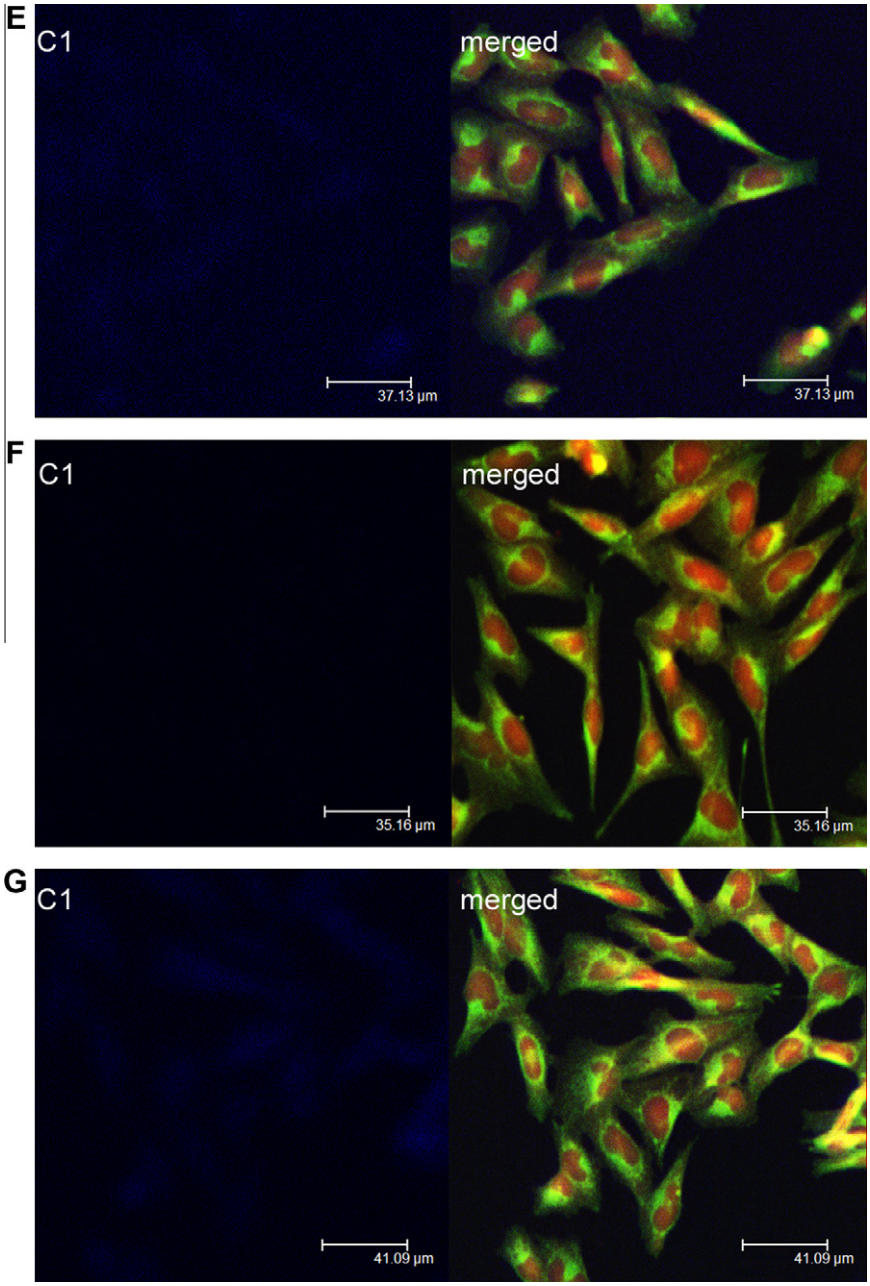

Fig. 3. (*continued*)

fluorescence-dye labeled COX-2 inhibitors, the intrinsic fluorescence of a 2,3-diarylsubstituted indole derivative alone was used to visualize COX-2 *in vitro*. Of note, C1 could be detected at very low concentrations, which were comparable to concentrations typically applied in radiotracer investigations [1]. A novel developed sample chamber that provides constant cryogenic temperatures (±1 K) is a prerequisite for this investigation. In this regard, cryofluorescence microscopy provides several advantages like less dynamic quenching resulting in higher fluorescence intensity [14], less photobleaching and higher fluorescence lifetime [15–18]. In particular, this favors the cryofluorescence microscopy methodology as a promising tool in melanoma research, since fluorescence quenching by melanins and autofluorescence of melanins often interfere with 'standard' fluorescence-based methods. However, in the present pilot study amelanotic melanoma cells containing only trace amounts of melanins were used. Another advantage of the method is the minimization of artifacts in sample preparation by very fast cryogenic immobilization [19–21]. Although this method in the first place does not allow for an *in vivo* optical imaging application there are many potential applications *in vitro*/*ex vivo*, e.g., histological examinations of tumor biopsies, including melanoma. On the other hand, at higher concentrations fluorescent 2,3-diarylsubstituted indole-based selective COX-2 inhibitors also provide potential application *in situ* in fluorescence-guided endoscopic diagnosis and surgical interventions, respectively. The combination of visualization with spectroscopy provides evidence that the detected signal is due to specific association of C1 with COX-2. However, by using other membrane stains than 5-hex, which provide spectral properties not interfering with those of C1, this approach could be further improved. The high lipophilicity of C1 (log*P* = 4.39, calculated with ALOGPS) results in a relatively high background signal due to unspecific enrichment in membranes. This could be overcome by synthesis of other fluorescent 2,3-diarylsubstituted indole derivatives.

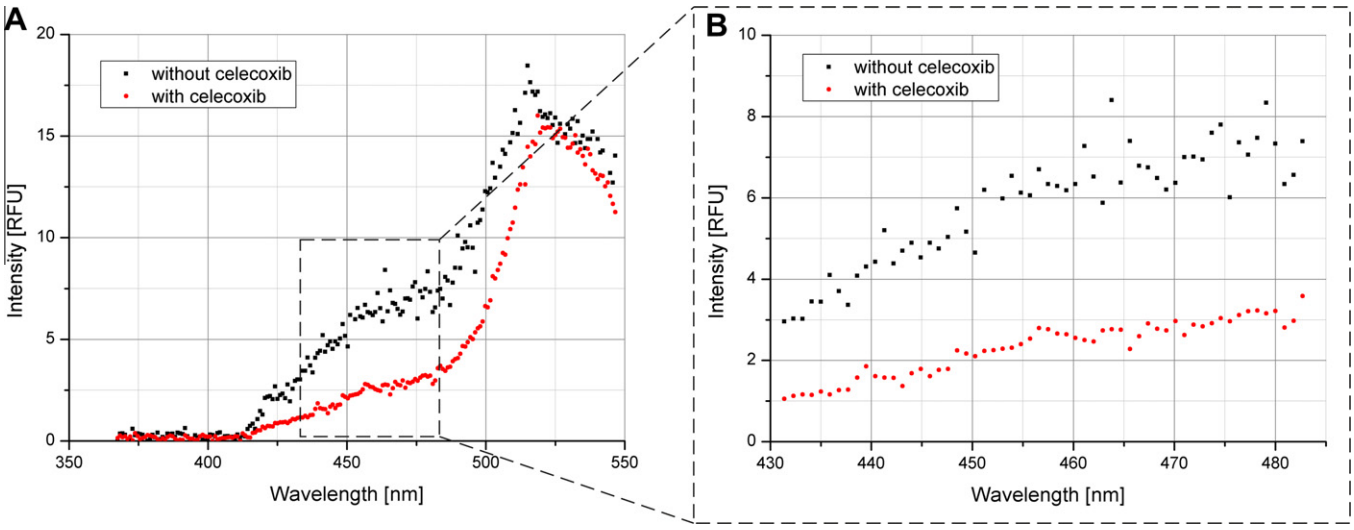

Fig. 4. Spectral data of the cellular uptake of C1 in A2058. Cells were incubated for 2 h with 1 nM C1 with (red) and without (black) celecoxib. (A) Whole spectrum, (B) set detection range (432–482 nm). (For interpretation of the references to color in this figure legend, the reader is referred to the web version of this article.)

4. Conclusions

The use of cryofluorescence microscopy at 20 K allowed for visualization of COX-2 protein expression in melanoma cells *in vitro* using a selective COX-2 inhibitor exhibiting intrinsic fluorescent properties. The compound applied is representative for a novel class of fluorescent 2,3-diarylsubstituted indole derivatives, which do not require additional chemical modification, e.g., by coupling to fluorescent dyes.

Acknowledgments

This work is part of research initiatives within the Helmholtz-Portfoliothema "Technologie und Medizin–Multimodale Bildgebung zur Aufklaerung des In-vivo-Verhaltens von polymeren Biomaterialien" and the Radiation-Induced Vascular Dysfunction (RIVAD) Research Network. Christin Wimmer is the recipient of a fellowship from the Europäische Sozialfonds (ESF).

References

[1] T. Kniess, M. Laube, R. Bergmann, F. Sehn, F. Graf, J. Steinbach, F. Wuest, J. Pietzsch, Radiosynthesis of a 18F-labeled 2,3-diarylsubstituted indole via McMurry coupling for functional characterization of cyclooxygenase-2 (COX-2) *in vitro* and *in vivo*, Bioorg. Med. Chem. 20 (2012) 3410–3421.
[2] C. Denkert, M. Köbel, S. Berger, A. Siegert, A. Leclere, U. Trefzer, S. Hauptmann, Expression of cyclooxygenase 2 in human malignant melanoma, Cancer Res. 61 (2001) 303–308.
[3] M.R. Becker, M.D. Siegelin, R. Rompel, A.H. Enk, T. Gaiser, COX-2 expression in malignant melanoma: a novel prognostic marker?, Melanoma Res 19 (2009) 8–16.
[4] W. Hu, Z. Guo, F. Chu, A. Bai, X. Yi, G. Cheng, J. Li, Synthesis and biological evaluation of substituted 2-sulfonyl-phenyl-3-phenyl-indoles: a new series of selective COX-2 inhibitors, Bioorg. Med. Chem. 11 (2003) 1153–1160.
[5] T.D. Penning, J.J. Talley, S.R. Bertenshaw, J.S. Carter, P.W. Collins, S. Docter, M.J. Graneto, L.F. Lee, J.W. Malecha, J.M. Miyashiro, R.S. Rogers, D.J. Rogier, S.S. Yu, G.D. Anderson, E.G. Burton, J.N. Cogburn, S.A. Gregory, C.M. Koboldt, W.E. Perkins, K. Seibert, A.W. Veenhuizen, Y.Y. Zhang, P.C. Isakson, Synthesis and biological evaluation of the 1,5-diarylpyrazole class of cyclooxygenase-2 inhibitors: identification of 4-[5-(4-methylphenyl)-3-(trifluoromethyl)-1H-pyrazol-1-yl]benzene-sulfonamide (SC-58635, celecoxib), J. Med. Chem. 40 (1997) 1347–1365.
[6] J.R. Lakowicz, Principles of Fluorescence Spectroscopy, Springer Science and Business Media, New York, USA, 2006.
[7] R. Kakkar, R. Garg, Suruchi, Theoretical study of tautomeric structures and fluorescence spectra of Hoechst 33258, J. Mol. Struct.: Theochem. 579 (2002) 109–113.
[8] B. Mosch, D. Pietzsch, J. Pietzsch, Irradiation affects cellular properties and Eph receptor expression in human melanoma cells, Cell Adh. Migr. 6 (2012) 113–125.
[9] D. Roscher, Dämpfungsanordnung für Tieftemperatur-Messzelle, DE 1020110165525, 2012
[10] T. Hla, K. Neilson, Human cycloocygenase-2 cDNA, PNAS 89 (1992) 7384–7388.
[11] L.J. Marnett, The COXIB experience: a look in the rearview mirror, Annu. Rev. Pharmcol. Toxicol. 49 (2009) 265–290.
[12] S.L. Timofeevski, J.J. Prisakiewicz, C.A. Rouzer, L.J. Marnett, Isoform-selective interaction of cyclooxygenase-2 with indomethacin amides studied by real-time fluorescence, inhibition kinetics, and site-directed mutagenesis, Biochemistry 41 (2002) 9654–9662.
[13] J. Uddin, B.C. Crews, A.L. Blobaum, P.J. Kingsley, D.L. Gorden, J.O. McIntyre, L.M. Matrisian, K. Subbaramaiah, A.J. Dannenberg, D.W. Piston, L.J. Marnett, Selective visualization of cyclooxygenase-2 in inflammation and cancer by targeted fluorescent imaging agents, Cancer Res. 70 (2010) 3618–3627.
[14] E.J. Bowen, J. Sahu, The effect of temperature on fluorescence of solutions, J. Phys. Chem. 63 (1959) 4–7.
[15] A. Sartori, R. Gatz, F. Beck, A. Rigort, W. Baumeister, J.M. Plitzko, Correlative microscopy: Bridging the gap between fluorescence light microscopy and cryo-electron tomography, J. Struct. Biol. 160 (2007) 135–145.
[16] C.L. Schwartz, V.I. Sarbash, F.I. Ataullakhanov, J.R. McIntosh, D. Nicastro, Cryo-fluorescence microscopy fascilitates correlations between light and cryo-electron microscopy and reduces the rate of photobleaching, J. Microsc. 227 (2007) 98–109.
[17] W.E. Moerner, M. Orrit, Illuminating single molecules in condensed matter, Science 283 (1999) 1670–1676.
[18] M.A. Le Gros, G. McDermott, M. Uchida, C.G. Knoechel, C.A. Larabell, High-aperture cryogenic light microscopy, J. Microsc. 235 (2009) 1–8.
[19] P.K. Luther, M.C. Lawrence, R.A. Crowther, A method for monitoring the collapse of sections as a function of electron dose, Ultramicroscopy 24 (1988) 7–18.
[20] K. McDonald, Cryopreparation methods for electron microscopy of selected model systems, Methods Cell Biol. 79 (2007) 23–56.
[21] J.C. Gilkey, L.A. Staehelin, Advances in ultrarapid freezing for the preservation of cellular ultrastructure, J. Electron Microsc. Tech. 3 (1986) 177–210.